Arabian Journal for Science and Engineering (2022) 47:8081–8091
https://doi.org/10.1007/s13369-021-06079-4

RESEARCH ARTICLE-MECHANICAL ENGINEERING

Experimental Investigation on Off-Design Characteristics of R290 Rolling Piston Compressor

Yuande Dai[1] · Jiantao Qiu[1] · Xiangtao Han[2]

Received: 4 February 2021 / Accepted: 12 August 2021 / Published online: 23 August 2021
© King Fahd University of Petroleum & Minerals 2021

Abstract

The test platform of R290 rolling piston compressor is established to study the variation of performance parameters under different conditions, including volumetric efficiency (η_V), coefficient of performance (COP), cooling capacity (Q), electric power (W), exhaust temperature (t_d), electrical efficiency (η_{el}), comprehensive efficiency coefficient (η_{com}). With the increase in suction temperature (t_s), COP increases by 8.3% partly due to the increase in t_d; η_V increases slowly in the range of 0.86–0.87 (mainly affected by temperature coefficient); η_{el} and η_{com} increase by 3.2% and 5.6%, respectively. At variable compression ratio (π) conditions, with the decrease of P_e (VPe), COP decreases by over 25%, while with the increase of P_c (VPc), COP decreases by over 38%, which attributes to the different decline rates of W (decreasing slightly at VPe and increasing by over 30% at VPc); η_V decreases slowly (mainly affected by volume coefficient and temperature coefficient); η_{el} decreases with the increase of π; the decline rate of η_{com} at VPc is 2–3 times that at VPe, which indicates that the frequent fluctuation of P_c will lead to the significant decrease of η_{com}. This research provides experimental basis for the design and further improvement of R290 rolling piston compressor.

Keywords R290 · Rolling piston compressor · Off-design characteristics · Performance parameters · Household air conditioner

Nomenclature

π	Compression ratio
EV	Expansion valve
EEV	Electronic expansion valve
Q	Cooling capacity, [W]
W	Electric power, [W]
f	Frequency, [Hz]
t_{en}	Ambient temperature, [°C]
t_e	Evaporating temperature, [°C]
t_c	Condensing temperature, [°C]
t_s	Suction temperature, [°C]
t_{sc}	Subcooling temperature, [°C]
t_d	Exhaust temperature, [°C]
P_e	Evaporating (suction) pressure, [Mpa]
P_c	Condensing (exhaust) pressure, [Mpa]
COP	Coefficient of performance
w	Work per unit mass, [kJ kg^{-1}]
COP_0	Theoretical coefficient of performance
Vts	Variable suction temperature conditions
theo-q	Theoretical cooling capacity per unit mass, [kJ kg^{-1}]
t_{asc}	Temperature after subcooling, [°C]
VPe	Variable compression ratio (variable evaporating pressure) conditions
VPc	Variable compression ratio (variable condensing pressure) conditions
Vπ	Variable compression ratio conditions
η_V	Volumetric efficiency
η_{el}	Electrical efficiency
η_{com}	Comprehensive efficiency coefficient
V_{cc}	Power supply voltage of compressor, [V]
η_i	Indicated efficiency
η	Efficiency (η_V, η_{el} or η_{com})
λ_V	Volume coefficient
λ_P	Pressure coefficient

✉ Yuande Dai
dydncutg@qq.com

Jiantao Qiu
756736802@qq.com

Xiangtao Han
1356541733@qq.com

[1] School of Mechanical and Electrical Engineering, Nanchang University, Nanchang 330031, China

[2] Nanjing Wuzhou Refrigeration Group Co., Ltd, Nanjing 211100, China

λ_T	Temperature coefficient
λ_l	Leakage coefficient
λ_h	Reflux coefficient
q_m	Inspiratory mass flow, [kg s^{-1}]
v_{suc}	Inspiratory specific volume, [m^3 kg^{-1}]
theo-w	Theoretical work per unit mass, [kJ kg^{-1}]
theo-COP	Theoretical coefficient of performance
theo-h_{asc}	Theoretical enthalpy after subcooling, [kJ kg^{-1}]

1 Introduction

The use of both hydrochlorofluorocarbons (HCFCs) and hydrofluorocarbons (HFCs) in the world will gradually enter the period of reduction according to Montreal Protocol and Kigali Amendment [1, 2]. Therefore, natural refrigerants with zero ozone depletion potential (ODP) and low global warming potential (GWP), such as R290, have been considered as substitutes for HCFCs and HFCs in household air conditioners. With the support and guidance of relevant policies from various countries, the relationship between compressors and mainstream refrigerants will be increasingly close. Therefore, the development of compressor suitable for new refrigerants is also an important research direction.

Much research has been carried out to promote the market application of R290. Zhang et al. [3] analyzed the feasibility of R290 replacing R22 by comparing the thermo-physical properties of R290 and R22. The results are as follows. The standard boiling point, freezing point, critical temperature and other parameters of R290 are very close to R22. The mass charge of R290 is less than that of R22 in the same volume. Under the same evaporator load, both the suction and exhaust temperatures of R290 are lower than that of R22, which can decrease the irreversible losses by weakening the heat exchange between fluid and cylinders. The saturated vapor dynamic viscosity and saturated liquid dynamic viscosity of R290 are smaller than these of R22, which can reduce the friction loss between R290 and pipe wall. The latent heat of vaporization of R290 is 1.84 times that of R22, and the thermal conductivity of R290 is 1.75 times that of R22, which is helpful to reduce the size of heat exchanger and improve the overall performance of air conditioning system.

In the early phase, many scholars have done a lot of research on R290 from two aspects: phase change heat transfer [4–7] and expansion valve [8–10]. In terms of compressor, Zou et al. [11] charged R290 for linear compressor instead of traditional reciprocating compressor and conducted performance test and power consumption analysis of linear compressor. The results show that in order to improve the energy efficiency of linear compressor, it is necessary to optimize the performance coefficient of linear motor and reduce the fit clearance between piston and cylinder at the same time. Yuan et al. [12] compared the thermodynamic performance of R290, R32 and R22 by establishing a thermodynamic simulation model of the rolling piston compressor, which shows that the increase in suction superheat has a great impact on the R290 compressor. Wu et al. [13, 14] made experimental studies on the starting characteristics of the rolling piston compressor under the refrigeration and heating mode. The results show that the mixing viscosity of oil and refrigerant and the oil level of the compressor oil pan are within reasonable range after the R290 system is started, which ensures the stable start-up of air conditioning system. Pilla et al. [15] evaluated the compressor performance of the mixed refrigerant R290/R600a and estimated the temperature distribution during the operation. The results show that 60% R290 and 40% R600a have the best system performance. Chen et al. [16] tested the friction coefficient, bite force and wear amount of the sliding plate piston friction pair under the R290/mineral oil mixture combination under the sealed high-pressure environment and compared it with the R410A/POE oil mixture combination which is widely used at present. The results show that under the combination of R290/mineral oil mixture, the anti-wear ability of the compressor is enhanced, but the friction power consumption is also increased, which needs further improvement. Sotomayor et al. [17] established a simulation model of open piston compressor for automotive air conditioning based on the existing experimental data and simulated the operation of R1234yf and R290 compressors based on the simulation model of R134a, and the predicted values were in good agreement with the experimental values, which proved the applicability of the model to the study of new refrigerants. Cai et al. [18] simulated and analyzed the leakage characteristics of R290 rolling piston compressor and compared the leakage characteristics of R22 and R410A. The results show that compared with R22 and R410A compressors under the same conditions, R290 compressor needs smaller radial clearance to obtain higher efficiency. The reduction of mass charge must be accompanied by the decrease in lubricating oil. The oil-free compressor for solving the problem of compressor oil supply under low oil level has also been developed [19].

In order to further promote the use of R290 in room air conditioner, it is necessary to study the rolling piston compressor for R290. At present, there are few experimental studies on the off-design characteristics of R290 rolling piston compressor. The purpose of this study is to investigate the influence of multiple operating conditions on the performance parameters of the compressor. Combined with the properties of R290 and rolling piston compressor, the experimental results are analyzed, which provides thermodynamic reference for the design and improvement of R290 rolling piston compressor and promotes the efficient utilization of

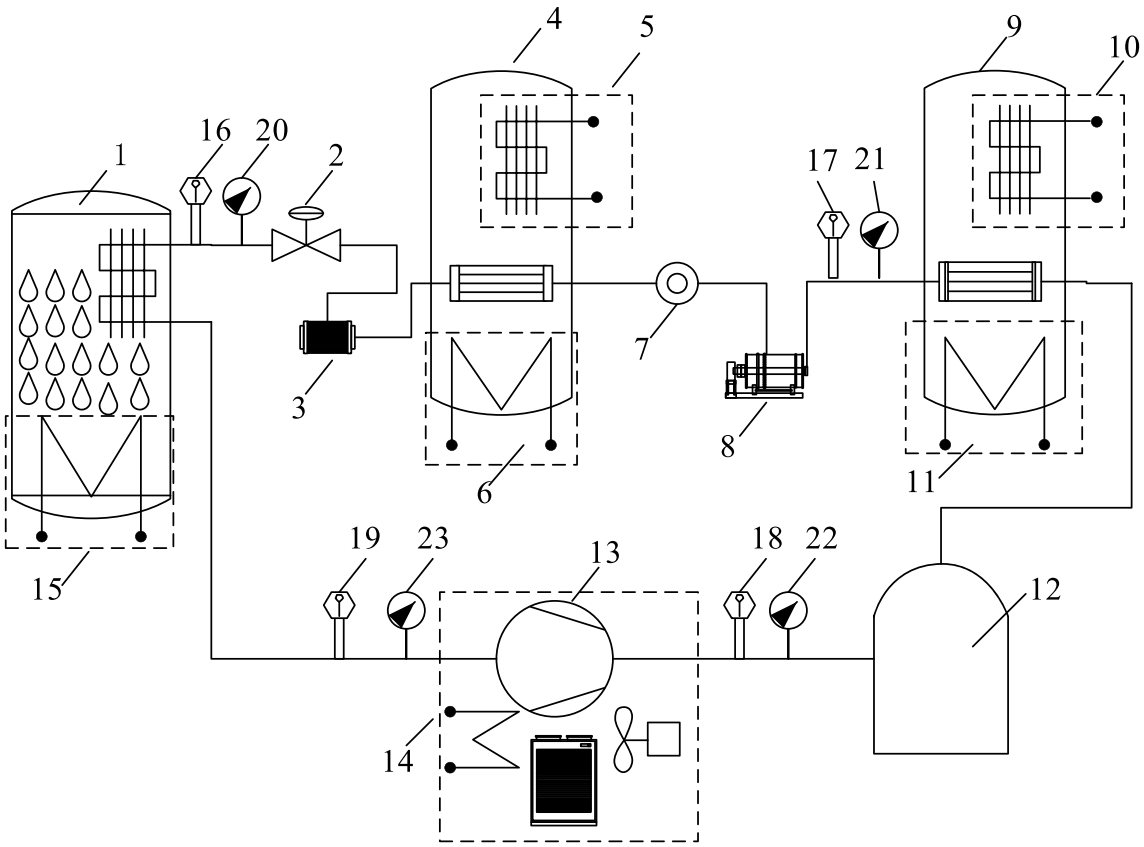

Fig. 1 The schematic diagram of system (1) Calorimeter. (2) Electronic expansive valve (EEV). (3) Filter. (4) Subcooler (water thermostat system). (5) Chiller for subcooler. (6) Electric heater for subcooler. (7) Visual liquid lens. (8) Dryer. (9) Condenser (water thermostat system). (10) Chiller for condenser. (11) Electric heater for condenser. (12) Oil separator. (13) Compressor. (14) Compressor environmental control room. (15) Electric heater for calorimeter. (16)–(19) Temperature sensor. (20)–(23) Pressure sensor

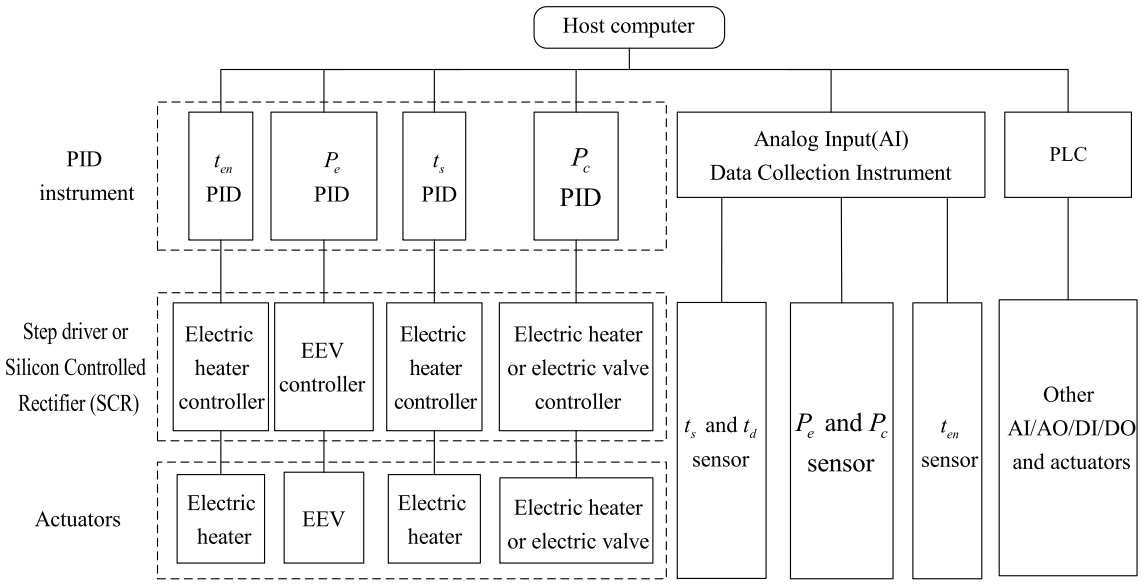

Fig. 2 Measurement and control schematic diagram of compressor test platform

R290. Through the performance test under variable operating conditions, it provides reference for the improvement of rolling piston compressors using R290 or other flammable refrigerants and promotes the commercialization of R290 rolling piston compressor.

2 Experimental Apparatuses and Operating Conditions

2.1 Descriptions of the Test Platform

In order to study the off-design characteristics of R290 rolling piston compressor, the test platform based on the secondary refrigerant calorimeter method [20] was set up. Figure 1 is the schematic diagram of system. After being compressed by the compressor, R290 (vapor) with high temperature and high pressure (exhaust pressure P_c) enters the oil separator, and the lubricating oil is separated. Then, R290 (vapor) enters the condenser for condensation and becomes liquid with medium temperature and high pressure. R290 (liquid) passes through the dryer and the visual liquid lens in turn and then enters the subcooler for subcooling. The supercooled R290 (liquid, responding to the temperature after subcooling t_{asc} and subcooling temperature t_{sc}) flows through the filter and then enters the electronic expansive valve. After being cooled and depressurized, it becomes low-temperature (evaporating temperature t_e) and low-pressure (suction pressure P_e) liquid. Then, it absorbs the heat of the secondary refrigerant in the calorimeter and turns into low-temperature and low-pressure R290 (vapor). Finally, it flows into the compressor (corresponding to the suction temperature t_s) for circulation.

The schematic diagram of the measurement and control for the test platform is shown in Fig. 2. The experimental parameters are adjusted by the refrigerating cycle system (e.g., Fig. 1) and the electrical measurement and control system (e.g., Fig. 2). For the monitoring and control of t_{en}, P_e, t_s, P_c and other important parameters, special PID instrument, actuators and drivers like step driver or silicon-controlled rectifier are used. For the control of other electrical components, programmable logic controller (PLC) is used for analog and digital control. To set the P_e (t_e) of the compressor, the opening of the electronic expansion valve (EEV) can be controlled by adjusting the output pulse of the special step driver, thus adjusting the mass flow of R290 and stabilize the P_e at the set value. The t_s of the compressor is controlled by monitoring the temperature of R290 at the outlet of the calorimeter (evaporator) in the refrigerating cycle system to control heat input by adjusting the power of electric heater in the calorimeter. While ensuring that the t_s reaches the set value, the sum of the heating amount of the electric heater and the heat leakage, and the heat absorption capacity of the evaporating coil achieve equilibrium. For the control of P_c, the condensing coil of the tested compressor system, an electric heater and a group of cooling water coils from another refrigerating cycle system are installed in a water thermostat system. The device achieves dynamic balance by controlling the electric heating capacity, the heat released by the cooling coil of another refrigerating cycle system and the condensing coil of the tested compressor system to maintain the constant P_c of the tested compressor. The control system of t_{sc} is basically the same as that of P_c control system, except that it monitors the t_{sc}. The PID control instrument receives the signal from the compressor ambient temperature (t_{en}) sensor and adjusts the operating frequency of the electric heater according to the error between the environmental setting value and the actual value, thus balancing the electric heating capacity and the cooling capacity of the fan coil air conditioning system. The voltage V_{cc} and frequency f of the compressor are controlled by the regulated power supply. Some known parameters of the tested compressor are shown in Table 1. The maximum allowable deviation between the measured value and the set value δ_{max} and the allowable deviation of the measured value relative to the average value δ_{avg} of the operating parameters in the experiment are shown in Table 2.

In addition, considering the flammability of R290, the corresponding adjustment and design of R290 rolling piston compressor are also made, such as the electronic joint of

Table 1 Some known parameters of the rolling piston compressor to be tested

Power supply parameters	Frequency	Displacement	Capacitance size/voltage	Height
1φ/220–240 V	50 Hz	24.2 cm^3	35μF/450 V	289.0 mm

Table 3 Compressor standard test conditions

t_c (℃)	t_e (℃)	t_{sc} (℃)	t_s (℃)	t_{en} (℃)
54.4 ± 0.3	7.2 ± 0.2	8.3 ± 0.2	35 ± 0.5/18.3 ± 0.5	35 ± 1

Table 2 Parameter error allowable settings

Category	P_e	t_s	P_c	t_{sc}	V_{cc}	f
δ_{max}	± 1%	± 3℃	± 1%	± 3.0%	± 3.0%	± 2.0%
δ_{avg}	± 0.5%	± 1℃	± 0.5%	± 2.0%	± 1.0%	± 1.0%

Table 4 Experimental conditions

Groups	No	t_s (℃)	t_e (℃)	P_e (MPa)	t_c (℃)	P_c (MPa)	π
Vts	1	15	7.2	0.588	54.4	1.883	3.2
	2	18.3	7.2	0.588	54.4	1.883	3.2
	3	22	7.2	0.588	54.4	1.883	3.2
	4	26	7.2	0.588	54.4	1.883	3.2
	5	30	7.2	0.588	54.4	1.883	3.2
	6	35	7.2	0.588	54.4	1.883	3.2
	7	41	7.2	0.588	54.4	1.883	3.2
VPe	8	18.3	12	0.673	54.4	1.883	2.79
	9	18.3	10	0.637	54.4	1.883	2.96
	10	18.3	7.2	0.588	54.4	1.883	3.2
	11	18.3	5	0.551	54.4	1.883	3.42
	12	18.3	3	0.519	54.4	1.883	3.63
	13	18.3	1	0.489	54.4	1.883	3.85
	14	35	12	0.673	54.4	1.883	2.79
	15	35	10	0.637	54.4	1.883	2.96
	16	35	7.2	0.588	54.4	1.883	3.2
	17	35	5	0.551	54.4	1.883	3.42
	18	35	3	0.519	54.4	1.883	3.63
VPc	19	18.3	7.2	0.588	46	1.569	2.67
	20	18.3	7.2	0.588	50	1.713	2.92
	21	18.3	7.2	0.588	54.4	1.883	3.2
	22	18.3	7.2	0.588	58	2.031	3.46
	23	18.3	7.2	0.588	60	2.117	3.75
	24	35	7.2	0.588	46	1.569	2.67
	25	35	7.2	0.588	50	1.713	2.92
	26	35	7.2	0.588	54.4	1.883	3.2
	27	35	7.2	0.588	58	2.031	3.46
	28	35	7.2	0.588	60	2.117	3.75

fireproofing design, which makes the compressor run more reliable; the special overload specially developed to avoid the danger of use; the special internal materials with good compatibility are used to effectively prevent aging, etc.

2.2 Descriptions of Operating Conditions

By controlling the parameters of operating conditions, the test conditions of compressor can be determined. The standard test conditions of compressor specified in GB/T 15765-2014 [21] are shown in Table 3. Based on the standard experimental conditions, in order to further study the off-design characteristics of R290 rolling piston compressor, the experimental conditions shown in Table 4 are designed by using the variable-controlling method. Conditions of No. 1–7 are variable suction temperature tests, which is called Vts; No. 8–28 are variable compression ratio tests called Vπ, in which No. 8–18 are variable compression ratio (variable evaporating pressure) tests called VPe and No. 19–28 are variable compression ratio (variable condensing pressure) tests called VPc. In addition, variable compression ratio conditions can be divided into two types: suction temperature of 18.3 ℃ and suction temperature of 35 ℃. As a measuring parameter of the system, t_{sc} is not the test condition of the compressor and has no effect on several performance parameters, such as the volumetric efficiency of the compressor. Therefore, in this experiment, t_{sc} is set to be 8.3 ℃ in all conditions, and the f of the compressor is 50 Hz.

3 Data Processing

Electric power W, coefficient of performance COP, exhaust temperature t_d can be measured or calculated indirectly from the experiments. The measurement and calculation methods of the above parameters refer to the existing test standards and related literature of compressor [13, 14, 20, 21]. Cooling capacity Q is calculated by Eq. (1)

$$Q = \frac{Q_1 + Q_2}{2} \tag{1}$$

where Q_1 is the sum of the electricity input to the electric heater and the heat leakage of the calorimeter, and Q_2 is

the product of the actual mass flow rate and enthalpy difference of R290 at the inlet and outlet of the calorimeter. The detailed calculation methods for both are given in the references [20].

Volumetric efficiency η_V is a parameter describing the utilization degree of working volume of compressor cylinder, reflecting the volume loss caused by clearance volume, suction resistance, suction heating, vapor leakage and suction reflux [22], which can be calculated by Eq. (2)

$$\eta_V = \lambda_V \lambda_p \lambda_T \lambda_l \lambda_h \tag{2}$$

where λ_V is the volume coefficient, it can be calculated by empirical Eq. (3)

$$\lambda_V = 1 - c\left[(\pi)^{\frac{1}{\kappa}} - 1\right] \tag{3}$$

where c is the relative clearance volume, and κ is the expansion adiabatic index.

λ_P is the pressure coefficient, which indicates the influence of relative pressure loss on volumetric efficiency at the end of suction, it can be considered as 1 because the rolling piston compressor has no suction valve; λ_T is the temperature coefficient, which reflects the reduction of the vapor transmission volume caused by the heating of the gas inhaled by the compressor. Its size is equal to the ratio of the density outside the suction port and in the cylinder at the end of the suction; λ_l is the leakage coefficient, which is related to the compression ratio, compressor structure, lubricating oil, etc; λ_h is the reflux coefficient, which is approximately equal to 1 because of the small edge angle [22].

From the experimental point of view, η_V can also be calculated by Eq. (4)

$$\eta_V = q_{va}/q_{vt} = v_{suc} q_m/(V_0 f) \tag{4}$$

where q_m is the tested inspiratory mass flow of R290 compressor [kg s^{-1}]; V_0 is the theoretical displacement of the compressor [m^3]; f is the frequency of the compressor [Hz]; v_{suc} is the specific volume of R290 at the suction port of the compressor [m^3 kg^{-1}]; q_{va} is the actual volume flow of R290 compressor [m^3 s^{-1}], while q_{vt} is the theoretical volume flow of R290 compressor [m^3 s^{-1}].

Electric efficiency η_{el} is a parameter that characterizes the perfection degree of the input work of the motor used in the compressor, which is the product of indicative efficiency η_i, heating efficiency η_t, leakage efficiency η_l, mechanical efficiency η_m and motor efficiency η_{mo}. When it comes to indicated efficiency η_i, a mathematical analysis model is proposed in reference [22], which can be calculated by Eq. (5)

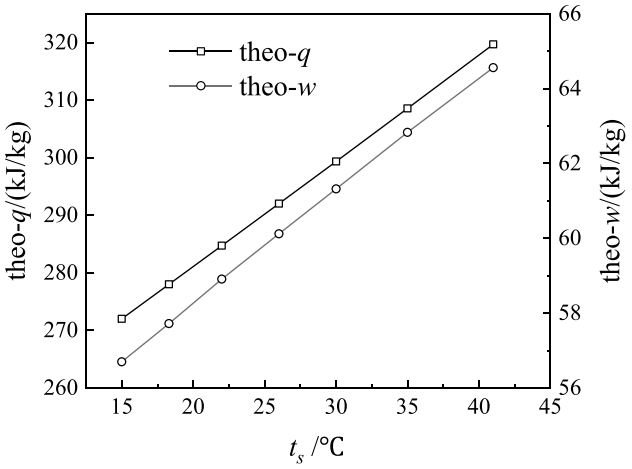

Fig. 3 Changes of theo-q, theo-w at Vts

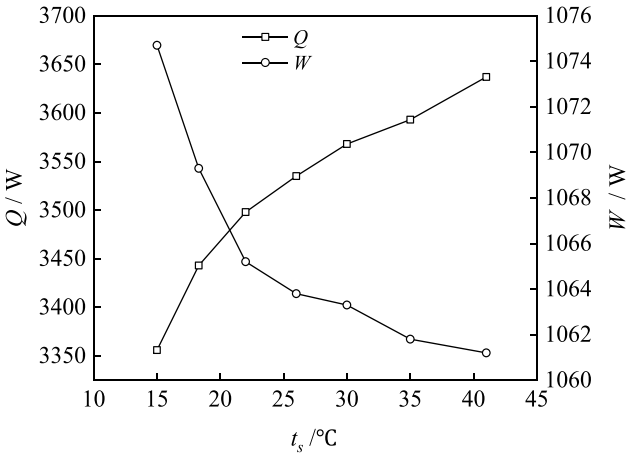

Fig. 4 Changes of Q, W at Vts

$$\eta_i = \frac{\lambda_T \lambda_l}{1 - \frac{1.5(\Delta p_{sm} + \Delta p_{dm} \pi^{1/\kappa})}{(h_{dis} - h_{suc})/v_{suc}}} \tag{5}$$

where Δp_{sm} and Δp_{dm} are the average pressure drop of suction and exhaust valves, respectively, Δp_{sm} can be ignored because there is no suction valve in rolling piston compressor; h_{suc} and h_{dis} are the specific enthalpies of suction and exhaust of compressor [kJ kg^{-1}]; π is the compression ratio; κ is the adiabatic index of R290.

Based on the experiment, the electric efficiency η_{el} is usually calculated by Eq. (6)

$$\eta_{el} = q_m\left(h_{dis,is} - h_{suc}\right)/W \tag{6}$$

where h_{suc} is the specific enthalpy of R290 at the suction port of the compressor [kJ kg^{-1}]; $h_{dis,is}$ is the specific enthalpy of isentropic compressed exhaust [kJ kg^{-1}].

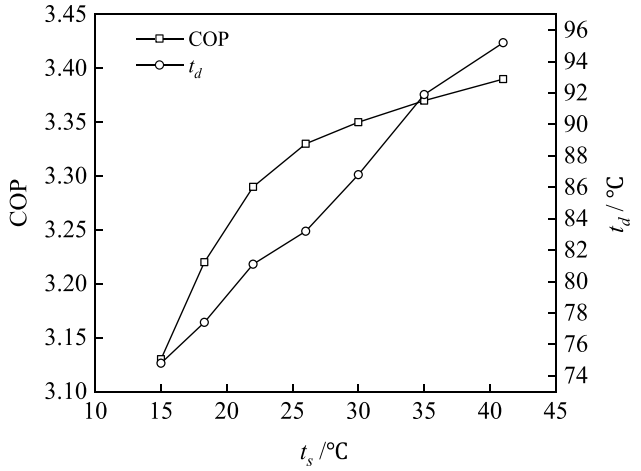

Fig. 5 Changes of COP, t_d at Vts

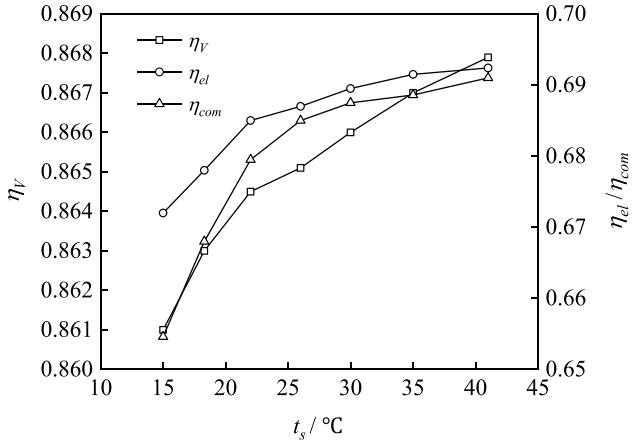

Fig. 6 Changes of η at Vts

Comprehensive efficiency coefficient η_{com} is the cycle efficiency, also known as the perfection degree of thermodynamics. It is usually calculated by Eq. (7)

$$\eta_{com} = \frac{COP}{COP_0} = \frac{COP}{(h_{suc} - h_{el})/(h_{dis,is} - h_{suc})} \quad (7)$$

where COP_0 is the theoretical coefficient of performance; h_{el} is the specific enthalpy at the inlet of evaporator [kJ kg^{-1}].

4 Results

4.1 Results at *Vts*

The superheat of this experiment is controlled by adjusting the power of the electric heater in the calorimeter, and the W is obtained by measuring the electric heating power, so the overheating belongs to useful superheat [23]. By consulting REFPROP version 10.0 [24], the unit mass cooling capacity (theo-q) and theoretical work per unit mass (theo-w) under the theoretical cycle are calculated, as shown in Fig. 3. It is worth mentioning that the pipeline resistance, suction and exhaust resistance and other factors are ignored in the theoretical cycle. When the t_s increases from 15 to 41 ℃, theo-q increases from 272 to 320 kJ/kg by 17.5%, while theo-w increases from 56.7 to 64.6 kJ/kg by 13.9%. Compared with the theoretical system, the changes of Q and W of R290 rolling piston compressor at Vts in the actual system are shown in Fig. 4. With the increase of t_s, Q increased from 3356 to 3637 W, an increase of 8.4%. It can be concluded that both Q and theo-q benefit from useful superheat. However, considering that with the increase of t_s, v_{suc} will increase, resulting in the decrease of q_m, so with the increase of t_s (especially 22 ℃), the growth rate of Q gradually slows down and lower than that of theo-q. Different from theo-w, W decreased from 1075 to 1061 W by 1.26%. The value of W is the product of q_m and w. Obviously, in this experiment, the effect of the decrease of q_m on W is greater than that of the increase of w, resulting in a small decrease of W. In conclusion, the Q increases, while the W decreases with the increase of t_s, and they both show a trend of slowing down when the t_s reaches 22 ℃.

In the theoretical system (in Fig. 3), the growth rate of theo-w is slightly lower than that of theo-q, which also leads to the increase of theo-COP by 3.22%. As shown in Fig. 5, with the increase of t_s, COP increases from 3.13 to 3.39 by 8.3%. However, the increase rate will gradually slow down when the t_s reaches 22 ℃. The reason for it is that the t_d also increases from 74.8 to 95.2 ℃ by 27.3% with the increase of t_s. Although in theory, the t_d of R290 is lower than some common refrigerants (like R22) at household air conditioning conditions, the t_d of the last two groups of experiments is above 90 ℃, which will have adverse effects on the operation of the system. If t_d is too high, it may bring about the decrease in viscosity of lubricating oil, cause poor lubrication, accelerate wear and increase power consumption. Meanwhile, high t_d will also reduce the cooling effect of exhaust on the motor. Therefore, when it comes to using R290 that is flammable in a refrigerating cycle system, we should try our best to avoid operating the system under the conditions with high t_d.

Figure 6 shows the trend of efficiency η at Vts. When t_s increases, η_V increases slowly in the range of 0.86–0.87. The reasons for the changes are as follows. According to Eq. (2), for rolling piston compressor, λ_P and λ_h are approximately equal to 1, whose effect on η_V is negligible. According to Eq. (3), when π is constant, λ_V causes little effect on η_V. For λ_T, the v_{suc} increases after being heated by the cylinder. Therefore, at the beginning of compression, the ratio of refrigerant density outside the suction port to that in the

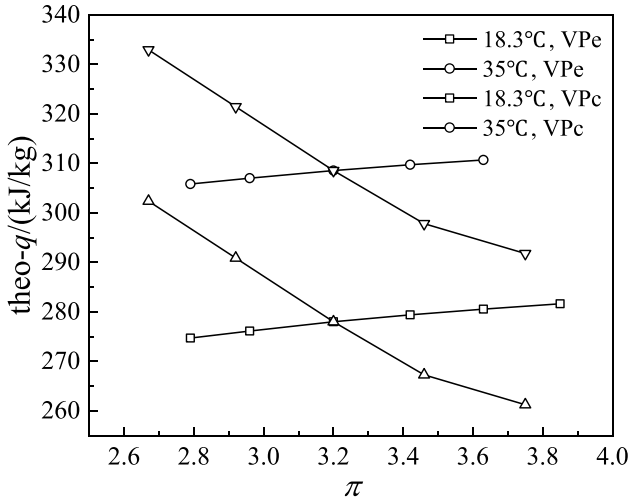

Fig. 7 Changes of *theo-q* at Vπ

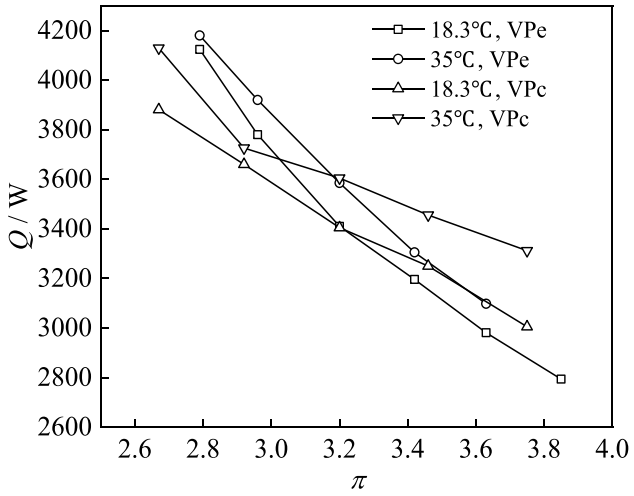

Fig. 9 Changes of *Q* at Vπ

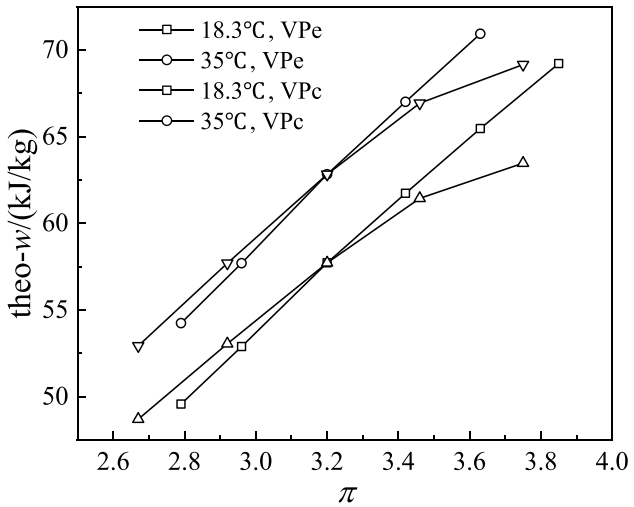

Fig. 8 Changes of *theo-w* at Vπ

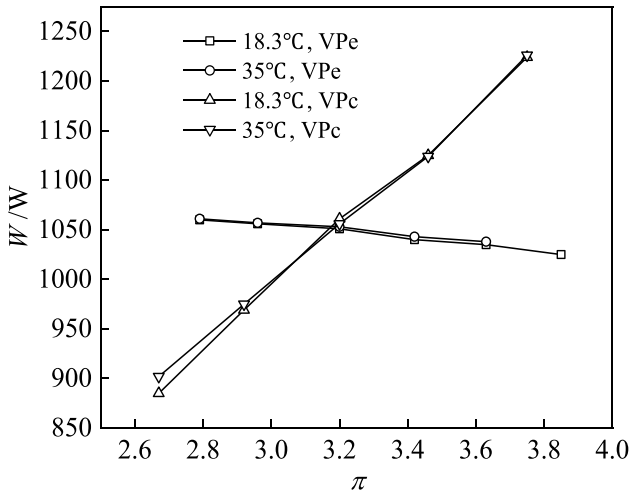

Fig. 10 Changes of *W* at Vπ

cylinder decreases at the end of compression suction, and λ_T decreases. However, with the increase of t_s, the temperature difference between the outside of the suction port and the inside of the cylinder decreases at the end of the compression suction, that is, the ratio of density increases and λ_T increases; For λ_l, R290 is in the vapor state when it is superheated, so there is no phenomenon that the liquid refrigerant dilutes the lubricating oil. Besides, the compression ratio remains unchanged, which basically has no effect on the refrigerant leakage of R290. Therefore, λ_l causes negligible effect on η_V. In general, η_V is mainly affected by λ_T and increases slightly. Obviously, the effective way to increase η_V is to increase t_s properly.

As shown in Fig. 6, η_{el} increases from 0.672 to 0.694, with an increase of 3.2%. The reasons can be analyzed from both theoretical formula and experimental results. First, when π is constant, with the increase of t_s, λ_l almost remains unchanged, while λ_T increases. Second, according to the experimental results and Eq. (5), the influence of the increase of λ_T and v_{suc} on η_i is greater than that of w on η_i, so η_{el} is increasing continuously. However, due to the increase of t_d, the cooling effect of exhaust on the motor is reduced, and the growth trend of η_{el} is gradually slowing down. With the increase of t_s, η_{com} increases from 0.655 to 0.691 by 5.6%. For the R290 rolling piston compressor system, the useful superheat promotes the growth of COP and COP_0. The increase in the ratio of the two indicates that the increment of COP is greater than that of COP_0. All in all, η increases with the increase of t_s and shows a trend of slowing down when the t_s reaches 22 ℃.

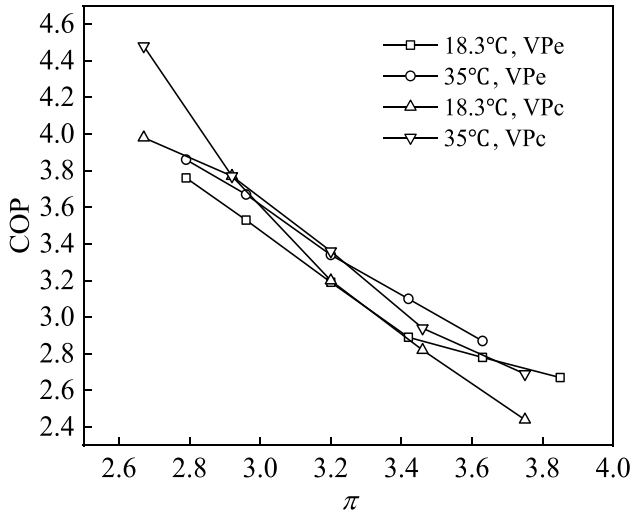

Fig. 11 Changes of COP at Vπ

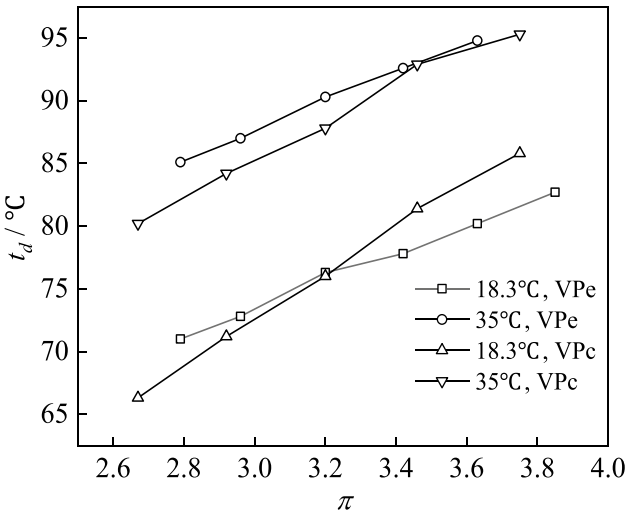

Fig. 12 Changes of t_d at Vπ

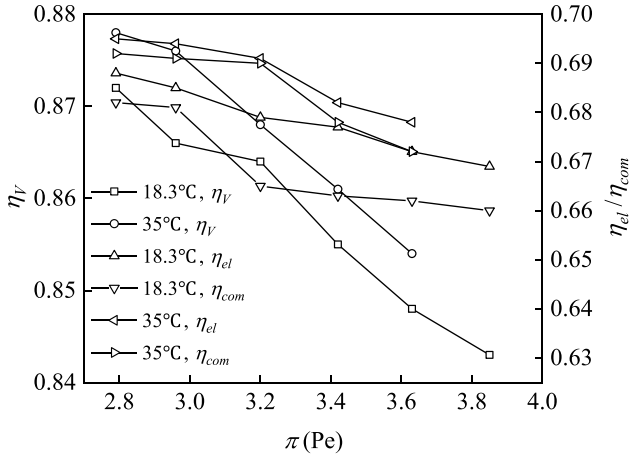

Fig. 13 Changes of η at VPe

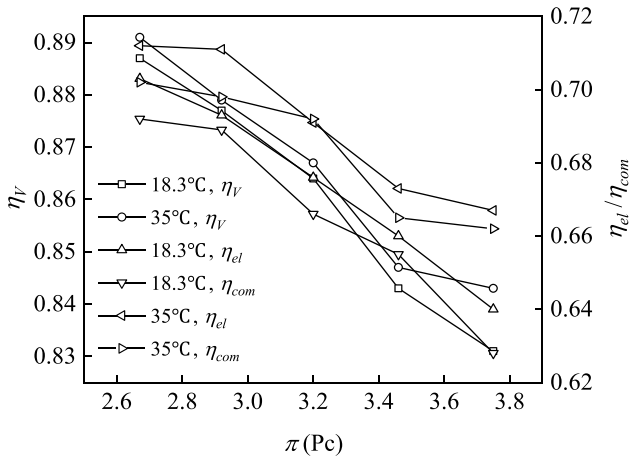

Fig. 14 Changes of η at VPc

4.2 Results at Vπ

Similar to Vts, theo-q and theo-w under Vπ were also studied theoretically. The variation of theo-q and theo-w under Vπ is shown in Figs. 7 and 8, respectively. With the decrease of P_e from 0.673 MPa to 0.519 MPa, theo-q at t_s of 18.3 ℃ increases from 274.7 to 280.6 kJ/kg by 2.1%, while theo-w at t_s of 18.3 ℃ increases sharply from 49.6 to 65.47 kJ/kg by 32.1%. By contrast, with the increase of P_c from 1.569 to 2.117 MPa, theo-q at t_s of 18.3 ℃ decreases from 302.4 to 261.2 kJ/kg by 13.6%, while theo-w at t_s of 18.3 ℃ increases sharply from 54.2 to 70.9 kJ/kg by 30.3%. It can be concluded that the effect of the increase of P_c on theo-q is greater than that of the decrease of P_e, which attributes to the increase in theoretical enthalpy after subcooling (theo-h_{asc}) when the P_c is increasing and the t_{sc} is constant. In addition, the growth trends of theo-q and theo-w at t_s of 35 ℃ are similar to those at t_s of 18.3 ℃.

Based on the analysis of the theoretical system, the changes of Q and W of tested R290 compressor at Vπ are shown in Figs. 9 and 10. With the decrease of P_e from 0.673 to 0.519 MPa, Q at t_s of 18.3 ℃ (35 ℃) decreases from 4124 (4180 W) to 2981 W (3098 W) by 27.7% (25.9%), while W at t_s of 18.3 ℃ (35 ℃) decreases slightly from 1060 (1061 W) to 1035 W (1038 W) by 2.4% (2.2%). With the increase of P_c from 1.569 to 2.117 MPa, Q at t_s of 18.3 ℃ (35 ℃) decreases from 3881 (4129 W) to 3005 W (3312 W) by 22.6% (19.8%), while W at t_s of 18.3 ℃ (35 ℃) increases from 885 (902 W) to 1224 W (1226 W) by 38.3% (35.9%). Obviously, different from theo-q at VPe, Q at Vπ shows a downward trend with the increase of π, and the variation range of Q is quite larger. The reason for it is that when the t_s is constant and P_e is decreasing, v_{suc} is constantly increasing,

greatly reducing the q_m and Q. Besides, different from theo-w at Vπ, with the increase of π, W at VPe decreases slightly, while W at VPc increases sharply, which indicates that compared with the decrease of P_e, the effect of the increase of P_c on W is much greater.

Figures 11 and 12 show the variation of COP and t_d of R290 rolling piston compressor system at Vπ, respectively. With the decrease of P_e, COP at t_s of 18.3 ℃ (35 ℃) decreases from 3.76 (3.86) to 2.78 (2.87) by 26.1% (25.7%). With the increase of P_c, COP at t_s of 18.3 ℃ (35 ℃) decreases from 3.98 (4.48) to 2.44 (2.73) by 38.7% (39.1%). When the t_s is 18.3 ℃, the decrease rate of COP at VPc is 48.5% higher than that at VPe, and the decrease rate is 52.3% higher when the t_s is 35 ℃, which mainly attributes to the difference of variation trend for W between VPe (decreased by about 2%) and VPc (increased by over 35%). On the other hands, with the decrease of P_e, t_d at t_s of 18.3 ℃ (35 ℃) increases from 71 (85.1) to 80.2 (94.8) by 13.0% (11.4%). With the increase of P_c, t_d at t_s of 18.3 ℃ (35 ℃) increases from 66.3 (80.2) to 85.8 (95.3) by 29.4% (18.8%). It can be concluded that the decline rate of t_d at VPc is 127.0% (95.2%) higher than that at VPe at t_s of 18.3 ℃ (35 ℃), and the increase of t_d is unfavorable to the operation of the system.

Figures 13 and 14 show the changes of η of R290 rolling piston compressor at Vπ. With the decrease of P_e, η_V at t_s of 18.3 ℃ (35 ℃) decreases from 0.872 (0.878) to 0.848 (0.854) by 2.8% (2.7%). With the increase of P_c, η_V at t_s of 18.3 ℃ (35 ℃) decreases from 0.887 (0.891) to 0.831 (0.843) by 6.3% (5.4%). The reasons for the changing trend of η_V are as follows. According to Eq. (3), λ_V increases with the increase of π. For λ_T, the v_{suc} increases after being heated by the cylinder. Therefore, at the beginning of compression, the ratio of density (R290) outside the suction port to that in the cylinder decreases at the end of compression suction, and λ_T decreases. However, when t_s is higher (35 ℃ compared to 18.3 ℃), the temperature difference between the outside of the suction port and the inside of the cylinder decreases at the end of the compression suction, that is, the ratio of density increases and λ_T increases slightly, which is the reason why the downward trend of η_V at t_s of 35 ℃ is lower than that of 18.3 ℃. For λ_l, R290 is vapor when it is overheated, so there is no phenomenon that the liquid refrigerant dilutes the lubricating oil. Although the leakage mainly depends on the structural clearance of the compressor, with the increase of π, λ_l will also decrease. In general, η_V decreases slightly with the increase of π.

With the decrease of P_e, η_{el} at t_s of 18.3 ℃ (35 ℃) decreases from 0.688 (0.695) to 0.672 (0.678) by 2.3% (2.5%). With the increase of P_c, η_{el} at t_s of 18.3 ℃ (35 ℃) decreases from 0.703 (0.712) to 0.640 (0.667) by 9.0% (6.3%). The reasons for the variation of η_{el} are as follows: The increase of π may increase the clearance value of the moving components of the compressor, reducing the mechanical efficiency; the increase of π will increase the t_d, weaking the cooling effect of the exhaust on the motor, thus reducing the motor efficiency. At VPe or VPc, the slope of the change curve of η_{el} under the condition of t_s of 35 ℃ is similar to that of 18.3 ℃, and the η_{el} of the former is greater than that of the latter (about 1.2% higher on average at VPe; 2.46% higher on average at VPc). In addition, it can be concluded that compared with the decrease of P_e, the increase of P_c has a greater impact on the decrease of η_{el}. With the decrease of P_e, η_{com} at t_s of 18.3 ℃ (35 ℃) decreases from 0.682 (0.692) to 0.662 (0.672) by 2.9% (2.9%). With the increase of P_c, η_{com} at t_s of 18.3 ℃ (35 ℃) decreases from 0.692 (0.702) to 0.628 (0.662) by 9.3% (5.7%). According to Eq. (7), the decrease of η_{com} mainly attributes to the significant decrease of COP, and the decreasing trend of COP was greater than that of COP_0. In addition, the decline rate of η_{com} at VPc is about 3 (2) times that at VPe at t_s of 18.3 ℃ (35 ℃). Therefore, avoiding the continuous fluctuation of P_c is an important measure to ensure the stability of η_{com}.

5 Conclusions

In this paper, the test platform of R290 rolling piston compressor was set up. The effects of t_s, π (P_e, P_c) on COP, Q, W, t_d, η_V, η_{el} and η_{com} of R290 rolling piston compressor were studied. Besides, the change laws were analyzed, and the following conclusions could be made from the experiments.

With the increase of t_s (from 15 to 41 ℃), Q increases from 3356 to 3637 W by 8.4%, while W decreases from 1075 to 1061 W by 1.26%, which attributes to the useful superheat and the decrease of q_m. Based on Q and W, COP increases from 3.13 to 3.39 by 8.31% although the increase rate will gradually slow down when the t_s reaches 22 ℃ because of the increase of t_d (increasing from 74.8 to 95.2 ℃ by 27.3%). For η, η_V increases slowly in the range of 0.86–0.87 (mainly affected by λ_T); η_{el} increases from 0.672 to 0.694 by 3.2%; η_{com} increases from 0.655 to 0.691 by 5.6%, which shows the improvement of performance at Vts (limited to the temperature range studied in this paper). In general, increasing t_s properly is an effective means to improve the performance of R290 rolling piston compressor.

With the decrease of P_e from 0.673 to 0.519 MPa, Q at t_s of 18.3 ℃ (35 ℃) decreases by 27.7% (25.9%), while W at t_s of 18.3 ℃ (35 ℃) decreases slightly by 2.4% (2.2%). With the increase of P_c from 1.569 to 2.117 MPa, Q at t_s of 18.3 ℃ (35 ℃) decreases by 22.6% (19.8%), while W at t_s of 18.3 ℃ (35 ℃) increases by 38.3% (35.9%), which shows that the downward trends of W at VPe and VPc are quite different. Meanwhile, the decline rate of t_d at VPc is 127.0% (95.2%) higher than that at VPe at t_s of 18.3 ℃ (35 ℃). For η, the downward trend of η_V at t_s of 35 ℃ is lower than that of 18.3 ℃ (mainly affected by λ_V and λ_T); η_{el} decreases

with the increase of π slightly (mainly depends on clearance value and the cooling effect of the exhaust on the motor); the decline rate of η_{com} at VPc is about 3 (2) times that at VPe at t_s of 18.3 ℃ (35 ℃), which indicates that the frequent fluctuation of P_c will lead to the significant decrease of η_{com}.

The construction of the experimental platform, the design of the experimental scheme and thermodynamic analysis of the changing trend of each variable provide thermodynamic and experimental references for the improvement of rolling piston compressor using R290 or other flammable refrigerants, promoting the commercialization of R290 rolling piston compressor. With that, the optimization of the suction and exhaust system of R290 rolling piston compressor is worth further research, which is closely related to the cooling capacity, electric power, volumetric efficiency, and the resistance in the flow process. The related structural improvement direction can focus on the thickness of the exhaust valve seat, the diameter of the exhaust hole, the height of the cylinder, etc. Based on these structural parameters, it is a good research method to use the simulation software to get the object with better performance and then carry out the whole machine experiment to verify the performance (such as cooling capacity and electric power) of the improved compressor.

Acknowledgements This research is sponsored by the National Natural Science Foundation of China (No. 22068024).

References

1. Shi, L.; An, Q.S.: Low GWP refrigerants options and countermeasures discussion after the entry into force of Kigali Amendment. Refriger. Air-Cond. **19**, 50–58 (2017)
2. Saeed, M.U.; Qureshi, S.R.; Hashmi, K.J.; Khan, M.A.; Danish, S.N.: Performance assessment of alternate refrigerants for retrofitting R22 based air conditioning system. Therm. Sci. **22**, 931–941 (2018)
3. Zhang, S.X.; Zhang, M.J.; Fu, Y.: Research on R290 as natural refrigerant in RAC. Electr. Appl. **1**, 41–46 (2010)
4. Li, K.Q.; He, G.G.; Jiang, J.K.; Li, Y.; Cai, D.H.: Flow boiling heat transfer characteristics and pressure drop of R290/oil solution in smooth horizontal tubes. Int. J. Heat Mass Transf. **119**, 777–790 (2018)
5. Wang, L.L.; Dai, Y.D.; Tian, S.Y.; Lin, Q.H.: Experimental investigation on characteristics of R290 boiling heat transfer in horizontal micro-fin tubes with small diameter. CIESC J. **71**, 1026–1034 (2020)
6. Dai, Y.D.; Guo, Y.J.; Zou, S.K.; He, G.G.: Experimental study on condensation heat transfer characteristics of R290 flowing in horizontal small tube. Acta Energ. Sol. Sin. **41**, 251–257 (2020)
7. Qiu, G.D.; Li, M.H.; Cai, W.H.: The effect of inclined angle on flow, heat transfer and mass charge of R290 condensation in a minichannel. Int. J. Heat Mass Transf. **154**, 119652 (2020)
8. Du, Y.J.; Wu, J.H.; Wang, C.; Chen, R.; Li, J.B.: Investigation on the influence of EEV opening on the reliability of an R290 ASHP during defrosting. Energy Build. **223**, 110218 (2020)
9. Li, J.B.; Du, Y.J.; Wu, J.H.; Lin, J.; Wang, C.: Experimental study on the failure of electronic expansion valve of a R290 split room air conditioner. Int. J. Refrig. **112**, 14–20 (2020)
10. Du, Y.J.; Wu, J.H.; Wang, C.; Li, J.B.: Experimental study on electronic expansion valve failure of a R290 room air conditioner during heating-defrosting process. Appl. Therm. Eng. **163**, 114432 (2019)
11. Zou, H.M.; Li, X.; Tang, M.S.; Shao, S.Q.; Tian, C.Q.: Experimental investigation on refrigeration performance of R290 linear compressor. CIESC J. **69**, 480–484 (2018)
12. Yuan, X.D.; Hu, J.S.; Song, Y.Q.; Jia, J.: Contrast study of thermodynamic performances for rotary compressor on R32 and R290. Cryog. Supercond. **46**, 75–80 (2018)
13. Wu, J.H.; Lin, J.; Zhang, Z.; Chen, Z.H.; Xie, J.; Lu, J.: Experimental investigation on cold startup characteristics of a rotary compressor in the R290 air-conditioning system under cooling condition. Int. J. Refrig. **65**, 209–217 (2016)
14. Wu, J.H.; Lin, J.; Zhang, Z.; Chen, Z.H.; Xie, J.; Lu, J.: Experimental investigation of dynamic characteristics of a rotary compressor and its air conditioner using R290 during warm startup. Appl. Therm. Eng. **125**, 1469–1477 (2017)
15. Pilla, T.S.; Sunkari, P.K.G.; Padmanabhuni, S.L.; Nair, S.S.; Dondapati, R.S.: Experimental evaluation mechanical performance of the compressor with mixed refrigerants R-290 and R-600a. Energy Procedia **109**, 113–121 (2017)
16. Chen, Z.H.; Li, G.M.; Wu, J.H.: Comparison of tribological characteristics of vane-piston interface between R290 and R410A in rotary compressor. J. Refriger. **39**, 1–6 (2018)
17. Sotomayor, P.O.; Parise, J.A.R.: Characterization and simulation of an open piston compressor for application on automotive air-conditioning systems operating with R134a, R1234yf and R290. Int. J. Refrig. **61**, 100–116 (2016)
18. Cai, D.H.; He, G.G.; Yokoyama, T.; Tian, Q.Q.; Yang, X.H.; Pan, J.: Simulation and comparison of leakage characteristics of R290 in rolling piston type rotary compressor. Int. J. Refrig. **53**, 42–54 (2015)
19. Wu, J.H.; Chen, Z.H.; Lin, J.; Li, J.B.: Experimental analysis on R290 solubility and R290/oil mixture viscosity in oil sump of the rotary compressor. Int. J. Refrig. **94**, 24–32 (2018)
20. Standardization Administration of China: GB/T 5773–2016: The Method of Performance Test for Positive Displacement Refrigerant Compressors. China Standards Press, Beijing (2016)
21. Standardization Administration of China: GB/T 15765–2014: Hermetic Motor-Compressors for Room Conditioners. China Standards Press, Beijing (2014)
22. Ding, G.L.; Zhang, C.L.: Simulation and Optimization of Refrigeration and Air Conditioning Equipment, p. 8–16. Science Press, Beijing (2001)
23. Lei, L.; Chen, H.; Guo, Y.; Zhou, K.; Fu, W.: Method of heating capacity test for compressor based on cooling capacity test device for compressor. Refriger. Air-Cond. **20**, 46-47+70 (2020)
24. Lemmon, E.W.; Huber, M.L.; McLinden, M.O.: NIST Standard Reference Database 23, NIST Reference Fluid Thermodynamic and Transport Properties. REFPROP version 10.0 (2018)